

AD-777 116

EFFECT OF BORON ADDITION ON THE
DIFFERENTIAL CAPACITANCE OF STRESS-
ANNEALED PYROLYTIC GRAPHITE

Jean-Paul Randin, et al

Case Western Reserve University

Prepared for:

Office of Naval Research

1 March 1974

DISTRIBUTED BY:

NTIS

National Technical Information Service
U. S. DEPARTMENT OF COMMERCE
5285 Port Royal Road, Springfield Va. 22151

AD-777116

OFFICE OF NAVAL RESEARCH

Contract N00014-67-A-0404-0006

Project NR 359-451

TECHNICAL REPORT NO. 36

EFFECT OF BORON ADDITION ON THE DIFFERENTIAL CAPACITANCE
OF STRESS-ANNEALED PYROLYTIC GRAPHITE

by

Jean-Paul Randin and Ernest Yeager

Department of Chemistry
CASE WESTERN RESERVE UNIVERSITY
Cleveland, Ohio 44106

1 March 1974



Reproduction in whole or in part is permitted for any
purpose of the United States Government

This document has been approved for public release
and sale; its distribution is unlimited

DOCUMENT CONTROL DATA - R & D

(Security classification of title, body of abstract and indexing annotation must be entered when the overall report is classified)

1. ORIGINATING ACTIVITY (Corporate author)		2a. REPORT SECURITY CLASSIFICATION	
Case Western Reserve University Cleveland, Ohio 44106		Unclassified	
3. REPORT TITLE		2b. GROUP	
EFFECT OF BORON ADDITION ON THE DIFFERENTIAL CAPACITANCE OF STRESS-ANNEALED PYROLYTIC GRAPHITE		---	
4. DESCRIPTIVE NOTES (Type of report and inclusive dates)			
Technical Report No. 36			
5. AUTHOR(S) (First name, middle initial, last name)			
Jean-Paul Randin and Ernest Yeager			
6. REPORT DATE		7a. TOTAL NO. OF PAGES	7b. NO. OF REFS
1 March 1974		25	
8a. CONTRACT OR GRANT NO.		9a. ORIGINATOR'S REPORT NUMBER(S)	
N00014-67-A-0404-0006		Technical Report No. 36	
b. PROJECT NO.		9b. OTHER REPORT NO(S) (Any other numbers that may be assigned this report)	
NR 359-451			
c.			
d.			
10. DISTRIBUTION STATEMENT			
This document has been approved for public release and sale; its distribution is unlimited			
11. SUPPLEMENTARY NOTES		12. SPONSORING MILITARY ACTIVITY	
----		Office of Naval Research Arlington, Virginia 22217 Code 472: Chemistry Program	
13. ABSTRACT			
<p>The non-faradaic differential electrode capacity of the basal plane of boronated stress-annealed pyrolytic graphite with 0.3 weight % boron has been studied in aqueous solution using an a.c. impedance bridge and compared to results previously obtained on the non-boronated material. On boronated graphite the potential of the minimum in the capacity-potential curve shifts negative by about 0.5 V relative to that for the non-boronated material. This shift is in agreement with the semiconductor interpretation proposed previously for the capacitance of the basal plane of the non-boronated material. The capacity of the minimum for the boronated material compares favorably with that estimated from the carrier concentration for the space charge region in the electrode phase.</p> <p>The potential of the minimum is essentially independent of pH over 14 units of pH for both the boronated and non-boronated material but the capacity potential curves for the former deviate substantially from the near parabolic shape found for the latter, particularly at potentials anodic to the capacity minimum. Boronation apparently introduces surface chemical groups which contribute to the observed capacity at these anodic potentials. With scans to potentials more anodic than 1 V vs. RHE, pronounced hysteresis effects are observed in the capacity-potential curves for the boronated material, probably because of the oxidation of the electrode surface.</p>			

Unclassified

Security Classification

14.	KEY WORDS	LINK A		LINK B		LINK C	
		ROLE	WT	ROLE	WT	ROLE	WT
	graphite electrodes boronated graphite semiconductors electrochemical capacity space charge regions						

Unclassified

Security Classification

TABLE OF CONTENTS

TITLE PAGE	i
DOCUMENT CONTROL DATA - R & D	ii
LIST OF FIGURES	v
INTRODUCTION	1
EXPERIMENTAL	2
RESULTS AND DISCUSSION	3
A. Behavior at potentials less anodic than 0.8V vs. RHE	3
B. Behavior on scanning to potentials more anodic than 1V vs. RHE	10
ACKNOWLEDGEMENT	13
REFERENCES	14
DISTRIBUTION LIST	20

LIST OF FIGURES

<u>Figure</u>	<u>Page</u>
1. Capacity-potential and current-potential curves for the basal plane of boronated stress-annealed pyrolytic graphite in 0.9 N NaF (pH \approx 6) at 25°C and 1000 Hz. Dashed curve for non-boronated stress-annealed pyrolytic graphite (1). Scan rate for the current-potential curve 0.1 V/sec, direction of sweep indicated by arrows.	15
2. Capacity-potential and current-potential curves for the basal plane of boronated stress-annealed pyrolytic graphite in 1N H ₂ SO ₄ (x) and in 1N NaOH (o) at 25°C and 1000 Hz. Dashed curve for non-boronated stress-annealed pyrolytic graphite in both 1N H ₂ SO ₄ and 1N NaOH (1). Scan rate for the current-potential curves 0.1 V/sec, direction of sweep indicated by arrows. A) 1N H ₂ SO ₄ ; B) 1N NaOH.	16
3. pH dependence of the electrode potential for the minimum and maximum capacity for the basal plane of boronated stress-annealed pyrolytic graphite at 25°C. o potential at the minimum capacity for the basal plane of boronated stress-annealed pyrolytic graphite. x potential at the minimum capacity for the basal plane of non-boronated stress-annealed pyrolytic graphite (1) (for comparison). o potential at the maximum capacity (peak at about +0.9 V vs. RHE) for the basal plane of boronated stress-annealed pyrolytic graphite. ----- 59 mV/pH slope (for comparison).	17
4. Capacity-potential and current-potential curves for the basal plane of boronated stress-annealed pyrolytic graphite in 0.9 N NaF (pH \approx 6) at 25°C and 1000 Hz. a) x measured with increasingly anodic potentials b) o measured with increasingly cathodic potentials c) Δ measured with increasingly anodic potentials Dashed curve for boronated stress-annealed pyrolytic graphite (1). Scan rate for the current-potential curves 0.1V/sec, direction of sweep indicated by arrows.	18
5. Capacity-potential and current-potential curves for the basal plane of boronated stress-annealed pyrolytic graphite in 1N H ₂ SO ₄ and 1N NaOH at 25°C and 1000 Hz, direction of sweep indicated by arrows. Scan rate for the current-potential curves 0.1V/sec. A) 1N H ₂ SO ₄ ; B) 1N NaOH	19

EFFECT OF BORON ADDITION ON THE DIFFERENTIAL CAPACITANCE
OF STRESS-ANNEALED PYROLYTIC GRAPHITE

INTRODUCTION

In previous publications (1-2), the non-faradaic differential capacity measured on the basal plane of high-pressure, stress-annealed pyrolytic graphite has been reported to have a near parabolic dependence on electrode potential with a minimum of about $3\mu\text{F}\cdot\text{cm}^{-2}$ in concentrated electrolytes. This low capacity value compared favorably with that estimated from the carrier concentration using the presently available theory of the space charge layer in semiconductor electrodes. Studies in NaF solutions at concentrations as low as 10^{-5}N indicated that in the range of potentials studied (+0.5 to -0.5 V vs. NHE), this minimum in the capacity vs. potential curve was not only associated with the diffuse ionic layer.

Further a.c. impedance measurements and linear sweep voltammetry have been carried out on boronated stress-annealed pyrolytic graphite to test the explanation proposed previously concerning the space charge contribution to the capacitance of the graphite/aqueous electrolyte interface.

Owing to the comparatively small density of states at the Fermi energy of pure graphite, electrically active impurities and defects are expected to alter very substantially the intrinsic properties of this material. Substitutional impurities such as boron can be incorporated uniformly and in controllable amount into the graphite matrix by diffusion at about 3000°C (3). Boron doping of graphite at levels higher

than about 1 atom % B results in a dispersion of boron carbides, B_4C , throughout the deposit, whereas at lower levels the boron atoms are introduced into substitutional trigonal sites in the graphite lattice (3,4).

Klein (3) has estimated the total charge carrier concentration in boronated stress-annealed pyrolytic graphite with 0.3 weight % boron to be $10 \times 10^{19} \text{ cm}^{-3}$, as compared to $1.2 \times 10^{19} \text{ cm}^{-3}$ for the undoped material (mean value from ref. 3, 5 and 6). Such a difference in carrier concentration between boronated and undoped pyrolytic graphite, associated with a change from an intrinsic to p-type semiconductor, makes the boronated graphite an interesting material for testing the semiconductor interpretation of the capacitance data.

EXPERIMENTAL

The boronated stress-annealed pyrolytic graphite used in this study^{a)} has an X-ray rocking curve whose mosaic spread width is 1.2° at half-maximum intensity of the (002) diffraction line, and a boron content of about 0.3 weight %. In the earlier work (1) with the undoped sample changes in the rocking angle in the range 0.4 to $\sim 8^\circ$ had practically no influence on the shape and minimum value of the capacity-potential curve. Consequently, it appears valid to compare the boronated sample with a 1.2° rocking angle studied in the present publication with the undoped material with a 0.4° rocking angle previously reported (1).

a) Supplied by the Union Carbide Technical Center Research, Parma, Ohio 44130.

As described earlier (1), a fresh electrode surface with the basal plane exposed was prepared for each experiment by placing a piece of plastic adhesive tape, cut to the exact size, in contact with the graphite surface and then peeling off a layer of graphite with the tape. The electrochemical system, the purifications of electrolytes and gas, and the instrumentation were the same as described earlier (1). All measurements were performed at $\sim 25^{\circ}\text{C}$.

All capacitances are given in terms of apparent electrode area. The ratio of the true-to-apparent area should be essentially unity for the basal plane of boronated stress-annealed pyrolytic graphite.

RESULTS AND DISCUSSION

The frequency dependence of the capacity measured for the boronated material is comparable to that previously reported (1) for the non-boronated stress-annealed pyrolytic graphite. The frequency dispersion is negligible provided the Teflon hood is slipped on to a freshly peeled dry electrode. All results reported in this study have been obtained in this manner.

A) Behavior at potentials less anodic than 0.8 V vs. RHE

The capacity-potential curve measured on the basal plane of boronated stress-annealed pyrolytic graphite in 0.9 N NaF ($\text{pH} \approx 6$) solution has no longer the near parabolic dependence on the electrode potential observed on the basal plane of the undoped graphite (see Fig. 1). Similar

results have been obtained for the boronated material in different electrolytes at several pH values. Capacity-potential curves obtained in 1N H_2SO_4 and in 1N NaOH are given in Fig. 2 , as well as results previously reported for the undoped graphite in the same electrolytes. The values in these figures were recorded point by point with potential increasing in the anodic direction. Within the potential range covered in Fig. 1 and 2, however, the capacity-potential curves measured point by point were essentially the same regardless of whether the data were obtained with increasing anodic or cathodic potentials.

Figures 1 and 2 indicate that the potential of the capacity minimum for the basal plane shifts towards more negative potentials by ~ 0.5 V relative to that of the non-boronated sample. The potential of this minimum is essentially independent of pH (see Fig. 3), as was also found for the basal plane of the non-boronated material, using the corresponding electrolytes. The impedance of the electrode interface was virtually pure capacitive at 1000 Hz in the vicinity of the capacitance minima in Figs 1 and 2. The series equivalent resistive component was below the precision of the bridge measurements after correction for the solution resistance.

The direction of the shift of the potential of the capacity minimum is in agreement with the semiconductor interpretation previously given (1,2) to explain the low capacitance of the graphite/electrolyte interface. The boronation of the graphite results in p-type semiconductor

characteristics and therefore should shift the potential of the capacity minimum towards more negative values relative to that observed for the basal plane of non-doped stress-annealed pyrolytic graphite.

For a p-type semiconductor with low doping and acceptors with energy level close to the band edges, the space charge capacity is given by the equation (7):

$$C_{sc} = \frac{\epsilon\epsilon_0}{L} \cdot \frac{|y(e^{-V_s} - 1) - y^{-1}(e^{+V_s} - 1)|}{\{[y(e^{-V_s} - 1) + y^{-1}(e^{+V_s} - 1) + (y - y^{-1})V_s]\}^{1/2}} \quad [1]$$

where the Debye length L is given by

$$L = \left[\frac{\epsilon\epsilon_0 kT}{2 n_i e_o^2} \right]^{1/2}$$

with ϵ = dielectric constant

ϵ_0 = vacuum permittivity

e_o = absolute value of elementary charge

k = Boltzmann constant

T = absolute temperature

V_s = $(\Delta\phi_s) e_o/kT$

$\Delta\phi_s$ = potential drop between the surface and bulk of the semiconductor

$$y = (p_o/n_i) = (n_i/n_o) = (p_o/n_o)^{1/2}$$

p_o = hole concentration in the bulk at equilibrium

n_o = electron concentration in the bulk at equilibrium

$$n_i = (n_o \cdot p_o)^{1/2} = \text{intrinsic carrier concentration}$$

Whereas the capacity minimum occurs at a potential drop across the space charge layer of $\Delta\phi_s = 0$ for an intrinsic semiconductor, the minimum is shifted for a p-type doped semiconductor to more cathodic potentials; for example, by $\Delta\phi_s \approx 60$ mV for $y = 10$. The electrode potential shift will correspond to this amount only if most of the change in electrode potential is across the space charge region within the semiconductor electrode.

Equation [1] is hardly applicable to stress- annealed pyrolytic graphite either doped or undoped because of the high carrier concentration and high concentration of lattice defects. Nonetheless, this equation may give some idea of an upper limit for the shift in the potential of the capacity minimum to be expected for the boronated material, assuming most of the change in electrode potential occurs across the space charge region. According to equation [1], the increment of approximately 10 fold in the total carrier concentration (corresponding to $y \approx 10$) for the boronated material would be expected to produce a change of ~ 0.08 V in the potential of the capacity minimum. The observed potential shift is an order of magnitude greater. The most probable explanation is that most of the change in the potential of the capacity minimum occurs across the Helmholtz region as the result of surface

states.

Capacity-potential curves on boronated stress-annealed pyrolytic graphite exhibit a shoulder at potentials anodic to the capacity minimum. A similar shoulder has been previously reported for the basal plane of non-boronated annealed pyrolytic graphite with $\Delta\theta_{\frac{1}{2}} \approx 8^\circ$ (see Fig. 12, ref. 1), which suggests a similar origin for the shoulder for both materials. On non-boronated annealed pyrolytic graphite, the shoulder has been attributed to the effect of some microorientations decreasing the crystal perfection of the basal plane. On boronated stress-annealed pyrolytic graphite with $\Delta\theta_{\frac{1}{2}} \approx 1.2^\circ$ boron most likely distorts the planar resonance structure of the basal plane of graphite. The valencies of carbon are then satisfied at these defects on the basal plane by foreign function groups. A change in the charge of these surface states may occur over a relatively narrow range of potentials. This would result in a large change in the potential distribution across the electrode-solution interphase and hence may cause a substantial additional shift in the potential of the capacity minimum as well as a shoulder in the capacity-potential curve.

The series capacitances in Figs 1 and 2 for the boronated material and the corresponding data for the non-boronated material (1, 2) fall in the range 3 to $7\mu\text{F}\cdot\text{cm}^{-2}$ and hence the Helmholtz capacitance C_H makes a significant contribution to the measured values. Unfortunately C_H is not

known. In the absence of specific adsorption, however, a value of $C_H = \sim 20 \mu\text{F.cm}^{-2}$ seems a reasonable estimate.^(a) Assuming no surface state contribution, a concentrated electrolyte, and a simple series equivalent circuit

$$\frac{1}{C} = \frac{1}{C_{sc}} + \frac{1}{C_H} \quad [2]$$

the space charge capacitance within the boronated graphite, corresponding to the minimum value of $C = 4.5 \mu\text{F.cm}^{-2}$ in Fig. 1 or 2, should be $C_{sc} = 5.8 \mu\text{F.cm}^{-2}$. Taking $p_o \approx 10^{20} \text{ cm}^{-3}$ (3), $y = 10$ ($n_i = 10^{19} \text{ cm}^{-3}$) and $\epsilon = 3$ (9), eq. [1] predicts a minimum value of C_{sc} of $\sim 14 \text{ F.cm}^{-2}$ at a value of $V_s \approx 3$ or $\Delta\phi_{sc} \approx + 0.08 \text{ V}$.

For the non-boronated material the corresponding experimental value of C_{sc} corrected from eq. [2], assuming $C_H = 20 \mu\text{F.cm}^{-2}$, is $3.6 \mu\text{F.cm}^{-2}$ as compared to $4.5 \mu\text{F.cm}^{-2}$ for the value calculated from eq. [1], taking $n_o + p_o = 1.2 \times 10^{19} \text{ cm}^{-3}$ (mean value from ref. 3, 5 and 6), $y = 1$ and $\epsilon = 3$ (9). Thus the experimental value for the minimum capacity on the

-
- a) The interaction of the water at the interface with the aromatic structure of the basal plane is likely to be very small, compared to that for metal electrodes (8). Consequently, the organization of the solvent constituting the dielectric of the Helmholtz capacitance in the absence of specific adsorption may differ from that for metals with the result that the value of C_H may deviate from the usual $20 \mu\text{F.cm}^{-2}$ expected near and cathodic to the point of zero charge for the ionic double layer. The authors doubt, however, that C_H would be sufficiently small as to become the predominant quantity in the series equivalent circuit for the interfacial impedance.

non-boronate stress-annealed pyrolytic graphite compares favorably with the value predicted from eq. [1]. The comparison is less favorable for the boronated material, which is not surprising considering the strenuous assumptions involved in the calculation of C_{sc} with eq. [1].

The potential dependence of the capacitance, however, deviates very substantially from that predicted by eq. [1] for the boronated material even on the cathodic side of the minimum, remote to the potential region where the surface states are assumed to have a pronounced effect on the potential dependence. A similar situation exists for the unboronated material (1, 2). The most likely explanation is that at the high charge carrier concentrations involved in the stress-annealed graphite, the semiconductor theory upon which eq. [1] and similar equations are based fails. The lack of any appreciable bandgap with a low density of states at the Fermi level introduces serious complications in the application of the usual semiconductor theory to graphite. The hole and electron concentrations in the space charge region are assumed to follow Boltzmann statistics with their interaction strictly coulombic. Their bulk concentrations are already very high and even at small values of $|\Delta\phi_s|$, the hole or electron concentrations at the interface would reach impossibly high values according to these oversimplified treatments.

Slow linear sweep voltammetry on the basal plane of boronated stress-annealed pyrolytic graphite reveals a peak in the cathodic sweeps

at potentials in the range -0.4 V vs. NHE (Figs 1-2). Similar peaks have been reported previously for the basal plane of the non-boronated samples (Figs 3 and 9, ref. 1), but have not been associated with any corresponding abnormality in the capacity-potential curves. Explanations previously proposed (1) to account for the presence of the voltammetry peak on undoped graphite should also apply to the case of boronated material.

B. Behavior on scanning to potentials more anodic than 1 V vs. RHE

Another feature of boronated pyrolytic graphite is the appearance of peaks and hysteresis effects in the capacity-potential curves on or after scanning to potentials more anodic than about 1 V vs. RHE. As already mentioned in regard to Fig. 1, point by point measurements did not present a noticeable hysteresis in the potential range from -0.9 to 0.45 V vs. NHE. On extending the capacitance measurements to potentials more anodic than 0.5 V vs. NHE in 0.9 N NaF ($\text{pH} \approx 6$), a sharp peak is recorded in the capacity-potential curve (Fig. 4), proceeding in the anodic direction. This peak does not appear in subsequent scans in either the cathodic or anodic directions (curve b and c, Fig. 4). Furthermore, the cathodic scan from 1.1 V vs. NHE (curve b, Fig. 4) is different from the cathodic scan from less anodic potential (Fig. 1) and the next anodic scan (curve c, Fig. 4) is no longer the same as the preceding one (curve a). The anodic scan following that in which the peak at about 1 V vs. NHE has been recorded (curve c, Fig. 4) seems to exhibit two minima at potentials slightly shifted towards the negative direction with respect to i) the minimum observed in the first scan at about -0.5 V vs. NHE, and ii) the minimum corresponding to the non-boronated sample at ~ 0 V vs. NHE. For comparison, the results

obtained for the basal plane of undoped stress-annealed pyrolytic graphite are also represented in Fig. 4 (dashed line). The sharp peak present at about +0.6 V. vs. NHE for the basal plane of the boronated graphite is not observed for the undoped material.

The 0.9N NaF solutions (pH=6) were unbuffered and hence at least some of the hysteresis effects in the capacity-potential curves in Fig. 4 may have been caused by pH changes arising from small unidentified faradaic currents. The oxidation and reduction of solution phase impurities or water itself, as well surface groups at imperfections on the graphite basal plane could cause substantial pH changes near the electrode surface.

Peaks and hysteresis effects, however, were also observed in the 1N H₂SO₄ and 1N NaOH solutions after scanning to very anodic potentials even though appreciable changes in pH should not occur in these solutions (see Fig. 5). Only the first very anodic and the reverse scans of the capacity-potential curves have been given in Fig. 5, although the complex behavior discussed for the 0.9N NaF solution for further anodic scans has also been observed. Two peaks are observed during the first anodic scan, one of which is at ~1V vs. RHE in the 1N H₂SO₄ solution and one also at this same potential in the 1N NaOH solution.

The pH dependence of the potential of the peak observed in the first anodic scan in the capacity-potential curves is 60 mV/decade

with a pH independent reference electrode (see Fig. 3). The origin of this peak is most likely some oxidation process at the electrode surface with a 60 mV/pH potential dependence and involving a surface group. As indicated earlier, boron atoms at the graphite surface may result in surface imperfections on the basal plane structure and hence foreign oxidizable groups which are destroyed or desorbed at more anodic potentials. The data available from the present study are insufficient to establish the nature of such groups.

The voltammetry curves for the basal plane of the boronated pyrolytic graphite did not show any peaks or variations at potentials corresponding to the peak in the capacity-potential curves even in the first sweep in the anodic direction for the NaF, NaOH, or H₂SO₄ solutions. At potentials in the vicinity of 1 V vs. RHE, the apparent capacities estimated from the anodic and cathodic sweep current densities at a sweep rate of 0.1 V/sec are relatively constant with a value of $\sim 20 \mu\text{F} \cdot \text{cm}^{-2}$ for the NaOH, H₂SO₄, and NaF solutions. This value is considerably higher than that measured at 1000 Hz. Assuming the capacity peaks to be caused by a parallel capacitive component, then the change in the capacitive current in the linear sweep voltammetry measurements would have been quite small in the H₂SO₄ solution ($\sim 5\%$) and even smaller for the NaOH solution ($\sim 1\%$). For the NaF solution the change would be $\sim 30\%$ but the lack of pH control in the NaF solution would be expected to interfere with the observation of the peak in the voltammetry studies because of pronounced irreversibility with respect to the transport of hydronium or hydroxide ions.

ACKNOWLEDGEMENT

The authors are pleased to acknowledge the support of this research by the U.S. Office of Naval Research. One of us (J.-P.R.) thanks the Stiftung für Stipendien auf dem Gebiete der Chemie, Basel, Switzerland, for the award of a Research Fellowship. The authors also express appreciation to the Union Carbide Technical Center, Parma, Ohio and Dr. A. Moore of that laboratory for providing the boronated pyrolytic graphite used in this study.

REFERENCES

1. J.-P. Randin and E. Yeager, J. Electroanal. Chem., 36, 257 (1972).
2. J.-P. Randin and E. Yeager, J. Electrochem. Soc., 118, 711 (1971).
3. C.A. Klein, J. Appl. Phys. 33, 3338 (1962).
4. D.E. Soule, in "Proc. Fifth Conf. on Carbon", 1, 13, Pergamon Press, Oxford (1962).
5. C.A. Klein and W.D. Straub, Phys. Rev. 123, 1581 (1961).
6. C.A. Klein, Rev. Mod. Phys. 34, 72 (1962).
7. See eg., H. Gerischer in "Physical Chemistry", H. Eyring, D. Henderson, and W. Jost, eds., Vol. 9A, Academic Press, New York (1970) pp. 468-477.
8. I. Morcos, J. Chem. Phys. 57, 1801 (1972).
9. S. Ergun, J.B. Yasinsky and J.R. Townsend, Carbon, 5, 403 (1967).

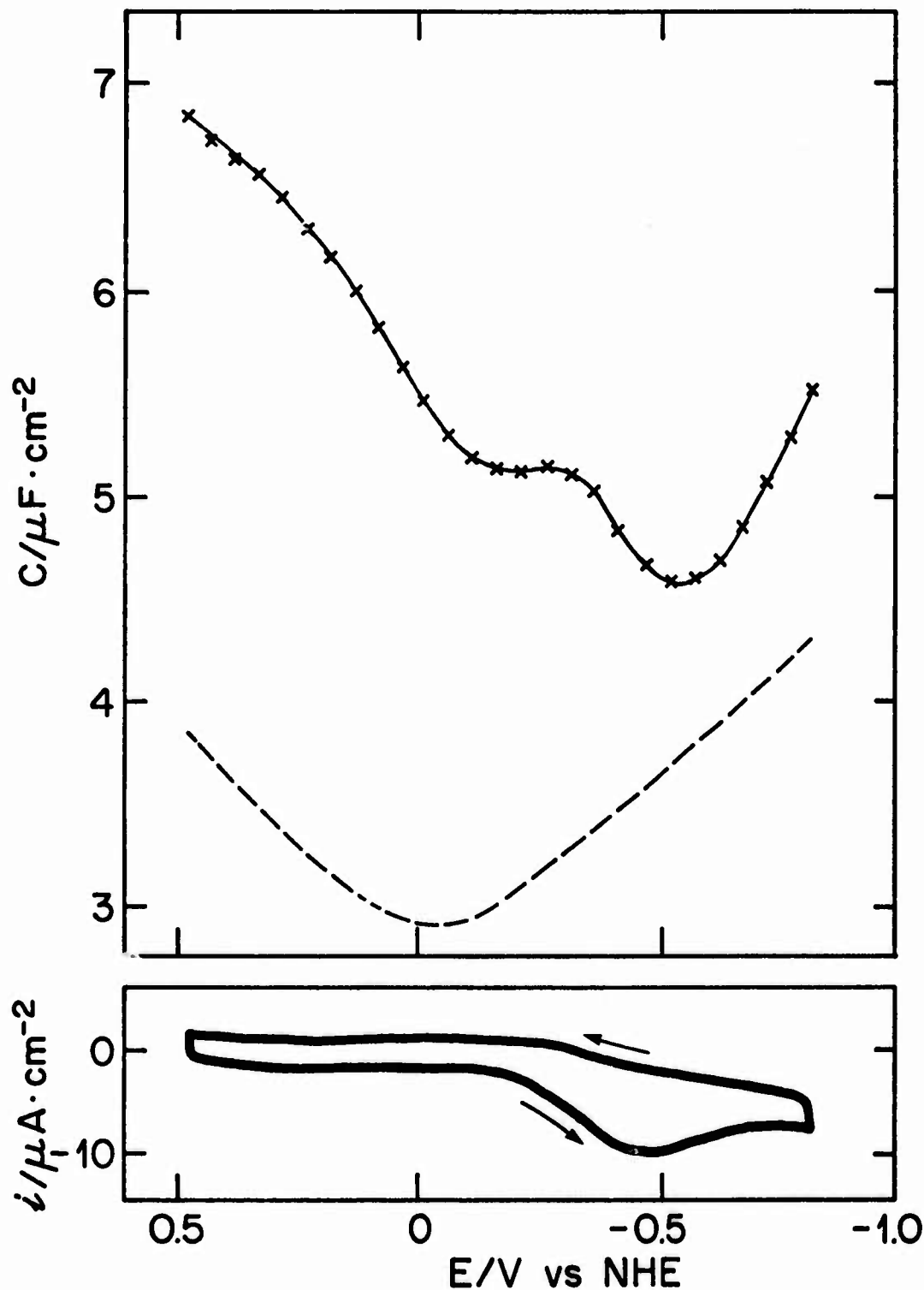


Figure 1. Capacity-potential and current-potential curves for the basal plane of boronated stress-annealed pyrolytic graphite in 0.9N NaF (pH=6) at 25°C and 1000 Hz. Dashed curve for non-boronated stress-annealed pyrolytic graphite (1). Scan rate for the current-potential curve 0.1V/sec, direction of sweep indicated by arrows.

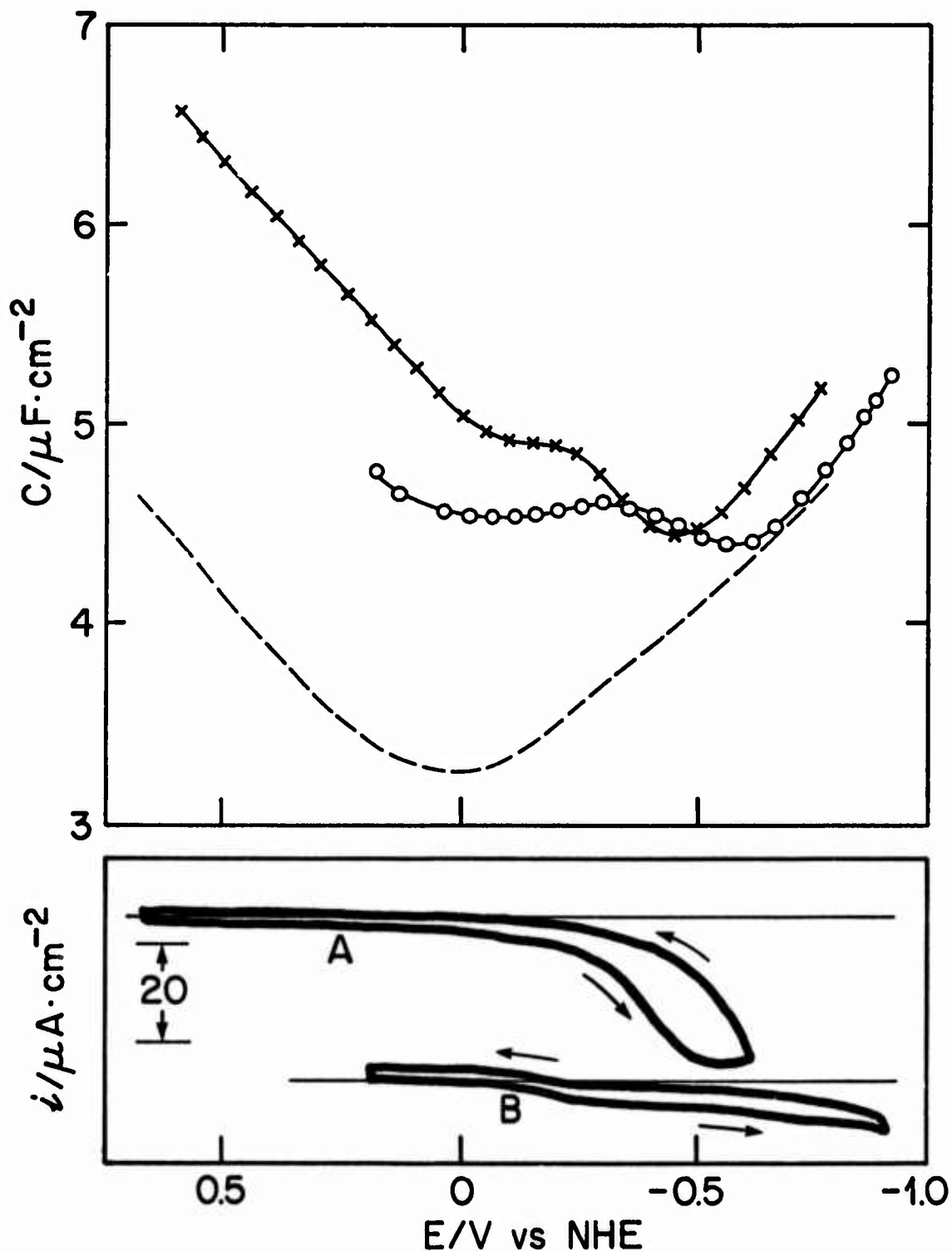


Figure 2. Capacity-potential and current-potential curves for the basal plane of boronated stress-annealed pyrolytic graphite in 1N H_2SO_4 (x) and in 1N NaOH (o) at 25°C and 1000 Hz. Dashed curve for non-boronated stress-annealed pyrolytic graphite in both 1N H_2SO_4 and 1N NaOH (1). Scan rate for the current-potential curves 0.1V/sec, direction of sweep indicated by arrows. A) 1N H_2SO_4 ; B) 1N NaOH.

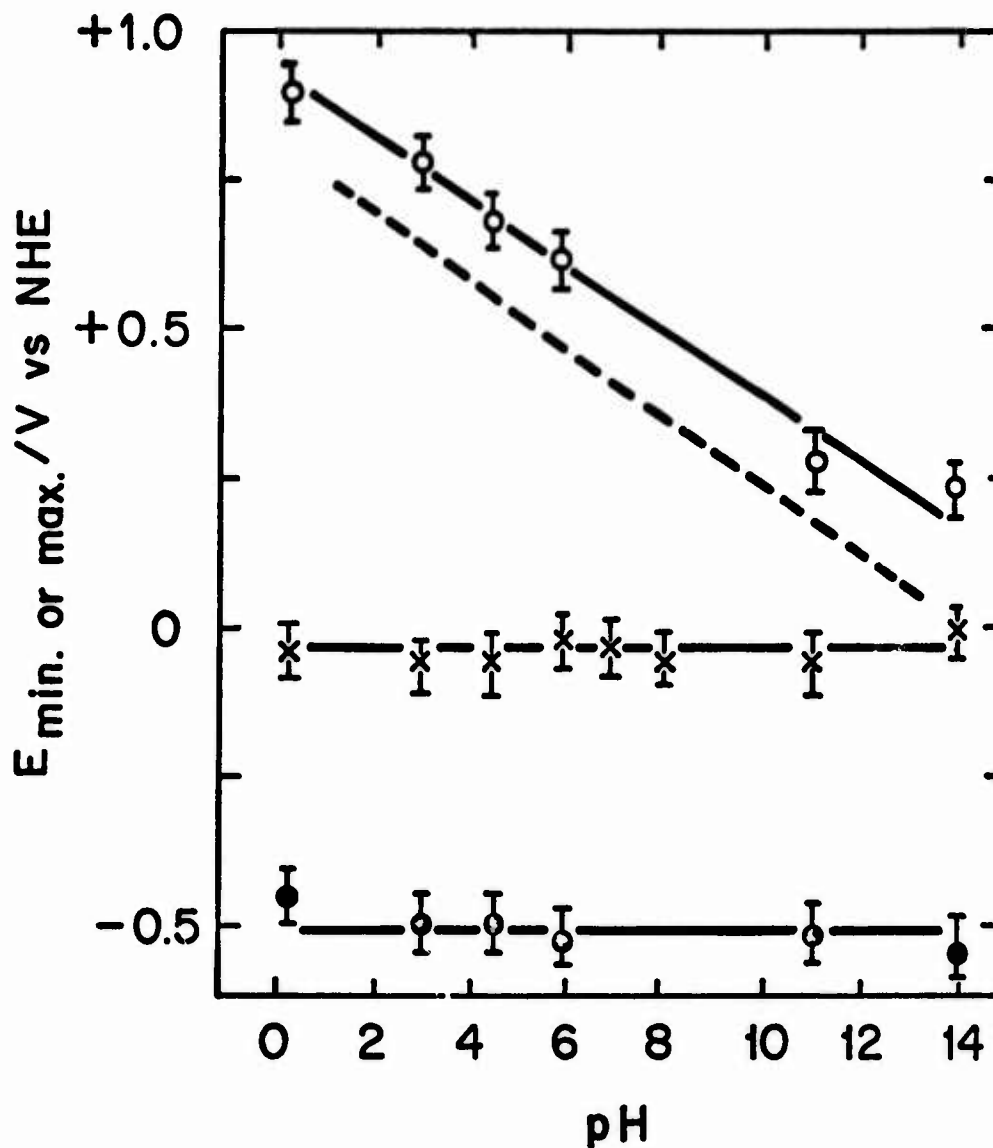


Figure 3. pH dependence of the electrode potential for the minimum and maximum capacity for the basal plane of boronated stress-annealed pyrolytic graphite at 25°C.

- potential at the minimum capacity for the basal plane of boronated stress-annealed pyrolytic graphite.
- x potential at the minimum capacity for the basal plane of non-boronated stress-annealed pyrolytic graphite (1) (for comparison).
- o potential at the maximum capacity (peak at about +0.9V vs. RHE) for the basal plane of boronated stress-annealed pyrolytic graphite.
- 59 mV/pH slope (for comparison).

Fig. 4

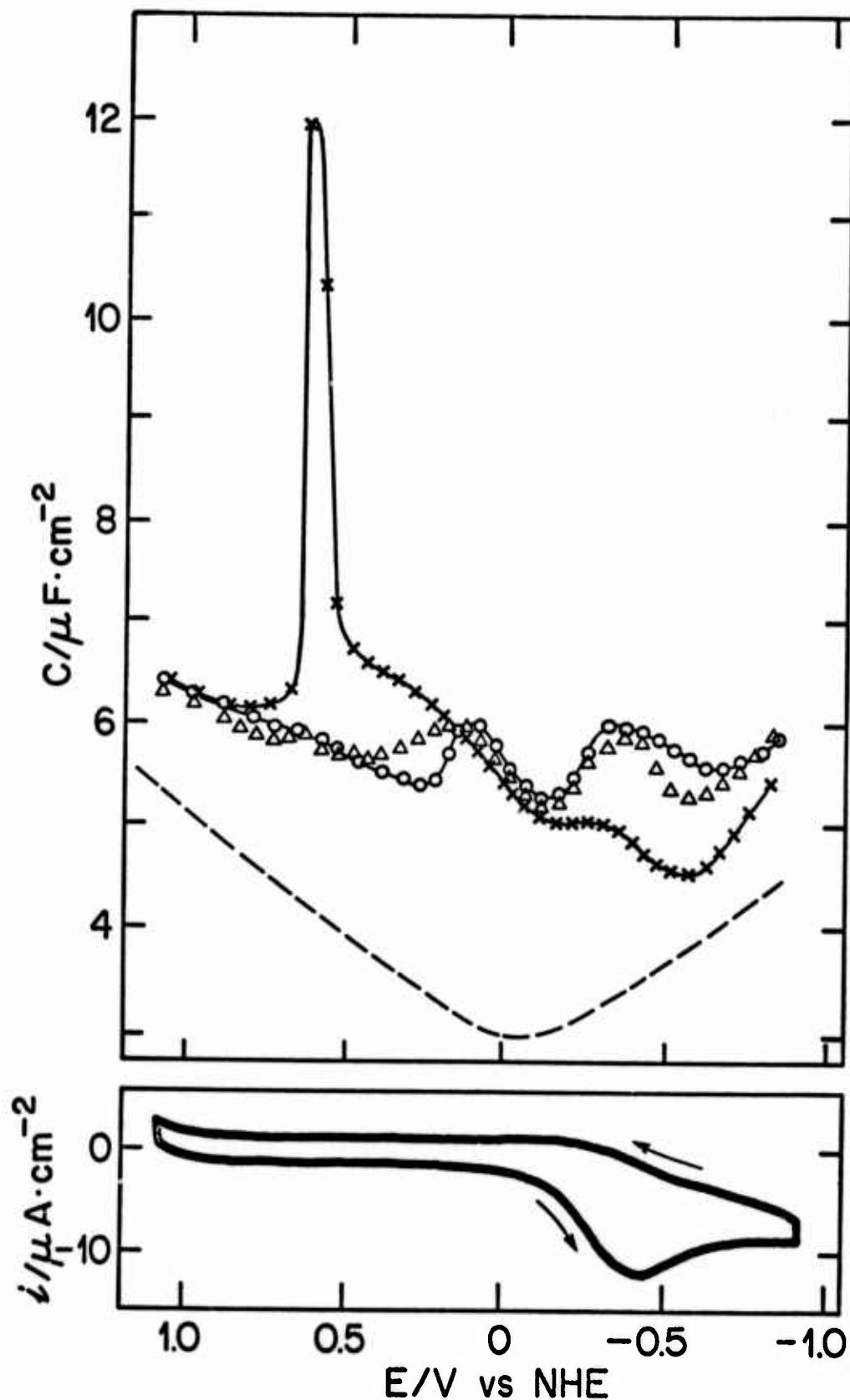


Figure 4. Capacity-potential and current-potential curves for the basal plane of boronated stress-annealed pyrolytic graphite in 0.9N NaF(pH=6) at 25°C and 1000 Hz.

- a) x measured with increasingly anodic potentials
- b) o measured with increasingly cathodic potentials
- c) Δ measured with increasingly anodic potentials

Dashed curve for boronated stress-annealed pyrolytic graphite (1). Scan rate for the current-potential curves 0.1V/sec, direction of sweep indicated by arrows.

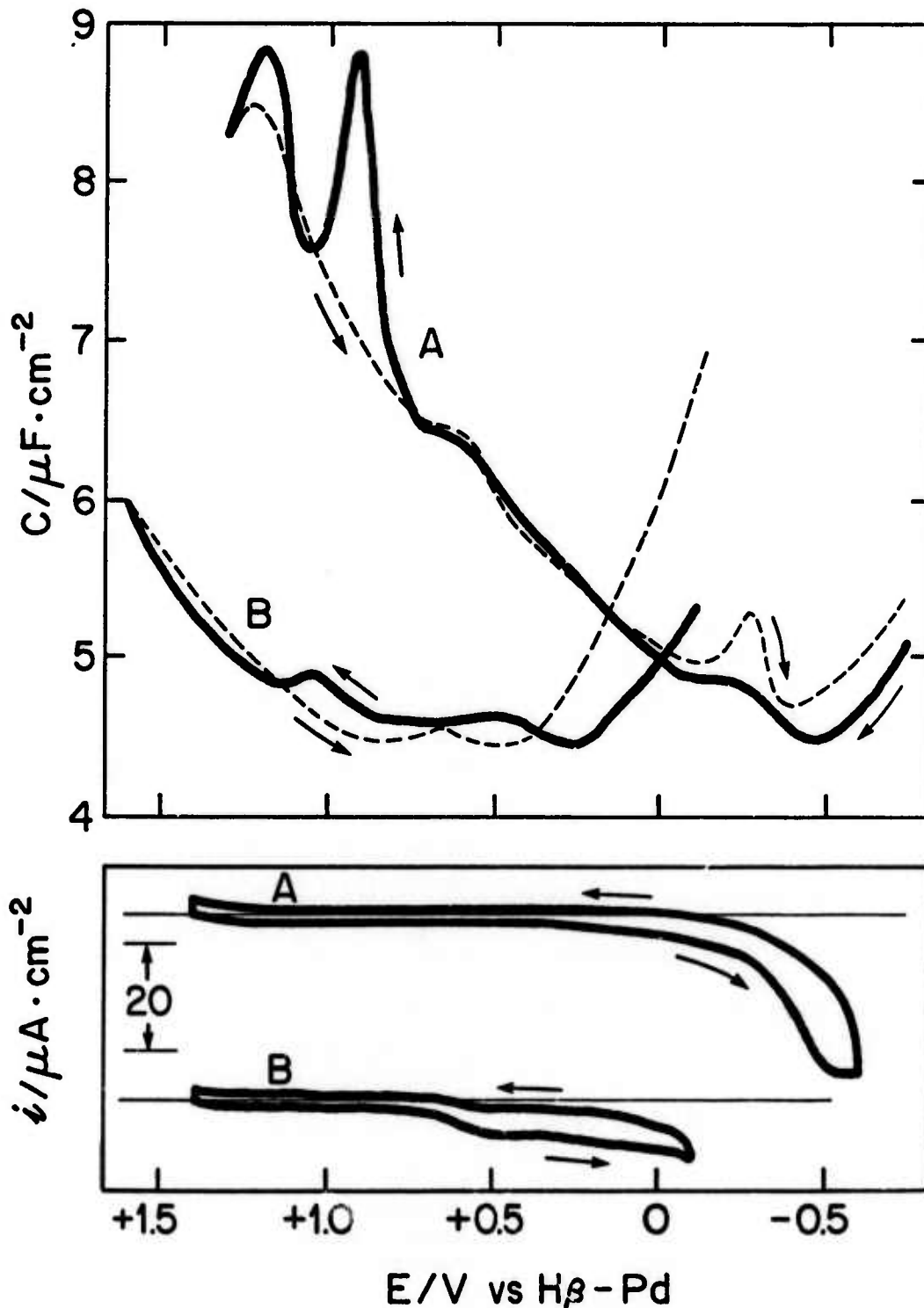


Figure 5. Capacity-potential and current-potential curves for the basal plane of boronated stress-annealed pyrolytic graphite in 1N H_2SO_4 and 1N $NaOH$ at 25°C and 1000 Hz, direction of sweep indicated by arrows. Scan rate for the current-potential curves 0.1V/sec.
A) 1N H_2SO_4 ; B) 1N $NaOH$